Mathematics

https://www.aimspress.com/journal/Math

AIMS Mathematics, 11(7): 23262–23281.
DOI: 10.3934/math.2026938
Received: 23 May 2026
Revised: 08 July 2026
Accepted: 14 July 2026
Published: 30 July 2026

Research article

EM algorithm in the slashed inverse Rayleigh regression model with an application

Héctor W. Gómez[1], **Diego I. Gallardo**[2], **Marcelo Bourguignon**[3] **and Osvaldo Venegas**[4,*]

[1] Departamento de Estadística y Ciencias de Datos, Facultad de Ciencias Básicas, Universidad de Antofagasta, Antofagasta 1240000, Chile

[2] Departamento de Estadística, Facultad de Ciencias, Universidad del Bío-Bío, Concepción 4081112, Chile

[3] Departamento de Estatística, Universidade Federal do Rio Grande do Norte, Natal 59078-970, RN, Brazil

[4] Departamento de Ciencias Matemáticas y Físicas, Facultad de Ingeniería, Universidad Católica de Temuco, Temuco 4780000, Chile

* **Correspondence:** Email: ovenegas@uct.cl.

Abstract: This paper introduced a novel distribution that generalized the inverse Rayleigh (IR) distribution. The proposed construction arose from the ratio of two independent random variables: one following the IR distribution and the other a beta distribution. Such a formulation yielded a more flexible model than the baseline IR distribution. We derived key distributional properties, proposed a regression model for the mean, and developed an expectation-maximization (EM) algorithm for maximum likelihood estimation. The finite-sample performance of the estimators was assessed via Monte Carlo simulations, and the practical utility of the model was illustrated through an application to real data.

Keywords: inverse Rayleigh distribution; slash distribution; maximum likelihood; quadratic variance function; EM algorithm
Mathematics Subject Classification: 62E15, 62F12, 62P99

1. Introduction

Recently, the slash-type methodology has been widely used to extend various distributions. In the case of the normal distribution, it can be represented as the ratio of two independent random variables: one normally distributed and the other following a Beta(q, 1) distribution. Under this formulation, we say that the resulting variable, denoted by V, follows a slash distribution if it can be written as

$$V = X_1/X_2, \tag{1.1}$$

where $X_1 \sim \mathrm{N}(0, 1)$, $X_2 \sim \mathrm{Beta}(q, 1)$, X_1 and X_2 are independent, and $q > 0$. The canonical slash distribution is obtained when $q = 1$, while the standard normal distribution is recovered as $q \to \infty$. The probability density function (PDF) of the canonical slash distribution is given by

$$g(x) = \begin{cases} \dfrac{\phi(0) - \phi(x)}{x^2}, & x \neq 0, \\ \dfrac{1}{2}\phi(0), & x = 0, \end{cases} \tag{1.2}$$

where ϕ denotes the standard normal density function (see Johnson et al. [1]). This distribution has heavier tails than the normal distribution; that is, it exhibits higher kurtosis. Properties of this family are discussed by Rogers and Tukey [2] and Mosteller and Tukey [3]. Maximum likelihood (ML) estimators for location and scale parameters are studied in Kadafar [4]. Wang and Genton [5] provide a multivariate version of the slash distribution as well as a skewed multivariate extension. Gómez et al. [6] and Gómez and Venegas [7] further extend the slash distribution and introduce the class of slash-elliptical distributions.

Several authors have extended asymmetric distributions with positive support using the slash methodology. For example, Gómez et al. [8] applied it to the Birnbaum-Saunders distribution; Olmos et al. [9, 10] applied it to the half-normal and generalized half-normal models (see Cooray and Ananda [11]); Astorga et al. [12] applied it to the generalized exponential model (see Mudholkar et al. [13]; Gupta and Kundu [14]); and Gómez et al. [15] applied it to the Gumbel model, among others.

Meanwhile, Treyer [16] proposed the IR distribution for reliability and survival data. Subsequently, Voda [17] observed that certain lifetime datasets from different experimental units could be approximated by the IR distribution. In addition, he studied certain properties of the ML estimator of the scale parameter of the IR distribution. A random variable X follows an IR distribution with scale parameter θ if its PDF is given by

$$f_X(x;\theta) = \frac{2\theta}{x^3}\exp\left(-\frac{\theta}{x^2}\right), \quad x > 0, \tag{1.3}$$

with $\theta > 0$, denoted by $X \sim \mathrm{IR}(\theta)$. The corresponding cumulative distribution function (CDF) is

$$F_X(x;\theta) = 1 - \exp\left(-\frac{\theta}{x^2}\right), \quad x > 0. \tag{1.4}$$

The IR distribution possesses only the first moment (mean); higher-order moments, including the variance, do not exist. The mean of $X \sim \mathrm{IR}(\theta)$ is given by

$$\mathbb{E}(X) = \sqrt{\pi\,\theta}, \tag{1.5}$$

and its first inverse moment is given by

$$\mathbb{E}(X^{-1}) = \frac{1}{2}\sqrt{\frac{\pi}{\theta}}. \tag{1.6}$$

Gharraph [18] studied several location measures of the IR distribution and investigated different estimation methods for its scale parameter. Mukherjee and Maiti [19] proposed a percentile-based estimator for the scale parameter, whereas Howlader et al. [20] and Soliman et al. [21] developed Bayesian inference procedures for the IR distribution. More recently, considerable attention has been devoted to extending the IR model in order to increase its flexibility. Representative examples include the half-logistic inverse Rayleigh distribution proposed by Almarashi et al. [22], the compound inverse Rayleigh distribution introduced by Chiodo et al. [23], the generalized inverse Rayleigh distribution of Bakoban and Al-Shehri [24], the transmuted lower record type inverse Rayleigh distribution introduced by Tanis [25], the modified inverse Rayleigh distribution proposed by Khan [26], and the three-parameter inverse Rayleigh distribution developed by Shala and Merovci [27]. In addition, the IR distribution has continued to find important applications in environmental and reliability analysis; for example, Chiodo and Di Noia [28] employed the classical IR distribution for stochastic modeling of extreme wind speeds under a Bayesian framework.

An important function for the new distribution is the generalized integro-exponential function, defined by the following integral representation (see Milgram [29]):

$$E_s^m(x) = \frac{1}{\Gamma(m+1)} \int_1^\infty (\log u)^m e^{-xu} u^{-s}\, du, \qquad x \in \mathbb{R}_+, \tag{1.7}$$

where $s \in \mathbb{R}^+$ and $m > -1$, Γ denotes the Gamma function, and log is the natural logarithm. In particular,

$$E_s^0(x) = E_s(x) = \int_1^\infty e^{-xu} u^{-s}\, du = x^{s-1} \int_x^\infty e^{-t} t^{-s}\, dt. \tag{1.8}$$

In many engineering and reliability applications, observed variables often exhibit substantial skewness, extreme observations, and heavier tails than those allowed by the classical inverse Rayleigh distribution. Examples include lifetime measurements, environmental indicators, and mining variables, where rare but large observations may occur. The slash methodology provides a simple mechanism to introduce additional tail flexibility via an extra shape parameter while preserving a tractable stochastic representation. Consequently, the proposed slash inverse Rayleigh (SIR) distribution can model a wider range of tail behaviors than the classical inverse Rayleigh model while retaining the IR model as a limiting case.

The main contributions of this paper can be summarized as follows.

(1) We introduce a new heavy-tailed extension of the IR distribution based on the slash methodology. The proposed model preserves the stochastic simplicity of the classical IR distribution while incorporating an additional shape parameter that controls tail behavior.

(2) We derive the principal mathematical properties of the proposed distribution, including its PDF, CDF, survival and hazard functions, stochastic representation, moments, limiting distribution, and regular variation properties.

(3) We formulate a regression model around the mean parameter and develop an efficient expectation-conditional maximization (ECM) algorithm for maximum-likelihood estimation. The hierarchical representation of the model allows computationally stable estimation without requiring direct maximization of the observed likelihood.

(4) We investigate the finite-sample performance of the proposed estimators through Monte Carlo simulations, showing satisfactory bias, root mean squared error (RMSE), and convergence properties.

(5) We demonstrate the practical usefulness of the proposed methodology through an application to mineral concentration data, where the proposed model provides a better fit than several well-established competing regression models.
(6) Furthermore, the paper establishes theoretical links between the proposed model and the classical IR distribution through mixture representations, limiting arguments, and tail characterization based on regular variation theory.

Unlike existing extensions of the IR distribution, the proposed model is obtained via a stochastic ratio representation, yielding closed-form expressions for several important probabilistic quantities while preserving computationally tractable likelihood-based inference.

The remainder of this paper is organized as follows. Section 2 presents the proposed distribution, including its representation, PDF, and some basic properties. In Section 3, we develop a regression model for the mean and propose an EM algorithm for parameter estimation via ML. Section 4 describes a simulation study conducted to assess the asymptotic behavior of the estimators. In Section 5, we present an application to a real mining dataset characterized by high skewness and kurtosis. Finally, Section 6 concludes the paper.

2. Density and properties

In this section, we introduce the representation, PDF, and properties of the new distribution.

2.1. Representation

The representation of this new distribution is given by

$$Z = \frac{X}{Y}, \tag{2.1}$$

where $X \sim \mathrm{IR}(\theta)$ and $Y \sim \mathrm{Beta}(q, 1)$ are independent, $\theta > 0$, $q > 0$, and the distribution of the random variable Z is called the SIR distribution. We denote this by $Z \sim \mathrm{SIR}(\theta, q)$.

2.2. Density function

The following proposition presents the PDF of the SIR distribution, obtained via the representation given in (2.1).

Proposition 1. *Let $Z \sim \mathrm{SIR}(\theta,\, q)$. Then, the PDF of Z is given by*

$$f_Z(z; \theta, q) = \frac{\theta q}{z^3} E_{q/2}\left(\frac{\theta}{z^2}\right), \quad z > 0, \tag{2.2}$$

where $\theta > 0$ is a scale parameter and $q > 0$ is a shape parameter.

Proof. Using the representation given in (2.1) and computing the Jacobian of the required transformation, we have that

$$\begin{Bmatrix} Z = \dfrac{X}{Y} \\ W = Y \end{Bmatrix} \Rightarrow \begin{Bmatrix} X = ZW \\ Y = W \end{Bmatrix} \Rightarrow J = \begin{vmatrix} \frac{\partial X}{\partial Z} & \frac{\partial X}{\partial W} \\ \frac{\partial Y}{\partial Z} & \frac{\partial Y}{\partial W} \end{vmatrix} = \begin{vmatrix} w & z \\ 0 & 1 \end{vmatrix} = w.$$

$$f_{Z,W}(z,w) = |J|\, f_{X,Y}(zw, w),$$
$$f_{Z,W}(z,w) = w f_X(zw)\, f_Y(w), \quad 0 < w < 1,\ z > 0,$$

so by marginalizing with respect to the random variable W, we obtain the density function corresponding to the random variable Z, namely,

$$f_Z(z;\theta,q) = 2q\theta \int_0^1 \frac{w^q}{(zw)^3} \exp\left(-\frac{\theta}{(zw)^2}\right) dw.$$

Making the variable transformation $u = (zw)^2$ and using (1.8), you get the result. □

Figure 1 shows the shape of the PDF for different values of q, considering $\theta = 1$. We observe that as the q parameter decreases, the right tail of the SIR distribution becomes heavier.

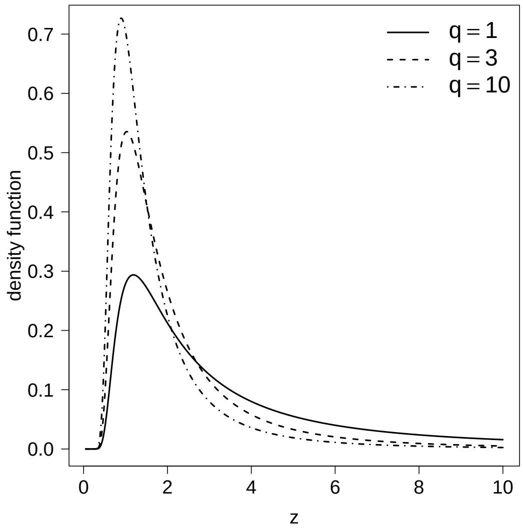

Figure 1. Plot of the SIR(1,q) distribution, for $q = 1$ (solid line), $q = 3$ (dashed line), $q = 10$ (dotted line).

2.3. Properties

In this subsection, we study basic properties of the SIR distribution.

Proposition 2. *Let $Z \sim \mathrm{SIR}(\theta, q)$. Then, the mode of Z is given as the solution of*

$$2\theta\, E_{q/2+1}\left(\frac{\theta}{z^2}\right) = 3z\, E_{q/2}\left(\frac{\theta}{z^2}\right). \tag{2.3}$$

Proof. Computing the first derivative of (2.2) with respect to z, the result follows. □

The following lemma is necessary to present the following proposition.

Lemma 1. *For $\theta > 0$, we have that*

$$\lim_{t\to 0} \frac{E_{q/2}\left(\frac{\theta}{t^2}\right)}{t^2} = 0. \tag{2.4}$$

Proof. Applying L'Hôpital's rule yields the result. □

Proposition 3. *Let $Z \sim \mathrm{SIR}(\theta, q)$. Then, the CDF of Z is given by*

$$F_Z(z;\theta,q) = \exp\left(-\frac{\theta}{z^2}\right) - \frac{z}{q} f_Z(z;\theta,q), \quad z > 0, \tag{2.5}$$

where $\theta > 0$ and $q > 0$.

Proof. Directly applying the definition of the CDF and (2.4) yields the result. □

The survival function $s(z)$, defined by $s(z) = 1 - F(z)$, for $Z \sim \mathrm{SIR}(\theta, q)$ is given by

$$s(z) = 1 - \exp\left(-\frac{\theta}{z^2}\right) + \frac{\theta}{z^2} E_{q/2}\left(\frac{\theta}{z^2}\right).$$

The hazard function $h(z)$, defined by $h(z) = \frac{f(z)}{s(z)}$, for $Z \sim \mathrm{SIR}(\theta, q)$ is given by

$$h(z) = \frac{\theta q\, E_{q/2}\left(\frac{\theta}{z^2}\right)}{z\left[\left(1 - \exp\left(-\frac{\theta}{z^2}\right)\right) z^2 + \theta\, E_{q/2}\left(\frac{\theta}{z^2}\right)\right]}, \qquad z > 0.$$

Figure 2 illustrates the hazard function's shape for selected values of q, assuming $\theta = 1$.

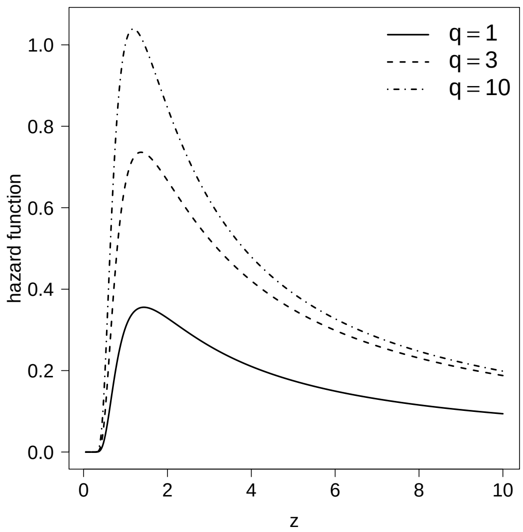

Figure 2. Examples of the hazard function for the SIR model for $q = 1$ (solid line), $q = 3$ (dashed line), $q = 10$ (dotted line).

Proposition 4. *Let $Z \mid Y = y \sim \mathrm{IR}(\theta y^{-2})$ and $Y \sim \mathrm{Beta}(q, 1)$. Then, $Z \sim \mathrm{SIR}(\theta, q)$.*

Proof. Directly computing the integral, we have

$$f_Z(z;\theta,q) = \int_{\mathrm{Rec}(y)} f_{Z|Y}(z) f_Y(y)\, dy = \int_0^1 \frac{2\theta y^{-2}}{z^3} \exp\left(-\frac{\theta y^{-2}}{z^2}\right) q y^{q-1}\, dy = 2\theta q \int_0^1 \frac{y^q}{(zy)^3} \exp\left(-\frac{\theta}{(zy)^2}\right) dy,$$

and making the change of variable $u = (zy)^2$ and using (1.8), we obtain the result. □

Proposition 5. *Let $Z \sim \mathrm{SIR}(\theta, q)$. If $q \to \infty$, then Z converges in distribution to a random variable* $\mathrm{IR}(\theta)$*.*

Proof. Let $Z \sim \mathrm{SIR}(\theta, q)$. Then, by the representation given in (2.1), we have $Z = \frac{X}{Y}$. We first study the convergence in probability of Y.

Since $Y \sim \mathrm{Beta}(q, 1)$, we have

$$\mathbb{E}[(Y-1)^2] = \frac{2}{(q+1)(q+2)}.$$

If $q \to \infty$, then

$$\mathbb{E}[(Y-1)^2] = \frac{2}{(q+1)(q+2)} \to 0,$$

which implies that $Y \xrightarrow{\mathcal{P}} 1$. Applying Slutsky's lemma yields the result. □

Remark 1. *The result of Proposition 4 shows that this SIR distribution is a scale mixture between the IR distribution and the Beta distribution. On the other hand, Proposition 5 indicates that as $q \to \infty$ in the SIR distribution, we obtain the IR distribution.*

Like the IR distribution, the SIR distribution has only the first moment; higher-order moments are not possible.

Proposition 6. *Let $Z \sim \mathrm{SIR}(\theta, q)$. Then, the first moment of Z can be written as*

$$\mu = \mathbb{E}(Z) = \frac{q\sqrt{\pi\theta}}{q-1}. \tag{2.6}$$

Proof. Using the stochastic representation for the distribution given in (2.1), we have that

$$\mu = \mathbb{E}(Z) = \mathbb{E}\left(\frac{X}{Y}\right) = \mathbb{E}(X)\,\mathbb{E}(Y^{-1}),$$

where

$$\mathbb{E}(Y^{-1}) = \frac{q}{q-1}, \qquad q > 1$$

and $\mathbb{E}(X) = \sqrt{\pi}\,\theta$ is the first moment of the $\mathrm{IR}(\theta)$ distribution given in (1.5). □

The following result will be necessary to find initial points in the estimation method.

Proposition 7. *Let $Z \sim \mathrm{SIR}(\theta, q)$. Then, the first inverse moment of Z can be written as*

$$\mu_{-1} = \mathbb{E}(Z^{-1}) = \frac{1}{2}\sqrt{\frac{\pi}{\theta}}\left(\frac{q}{q+1}\right). \tag{2.7}$$

Proof. Using the stochastic representation for the distribution given in (2.1), we have that

$$\mu_{-1} = \mathbb{E}(Z^{-1}) = \mathbb{E}\left(\frac{Y}{X}\right) = \mathbb{E}(Y)\,\mathbb{E}(X^{-1}),$$

where

$$\mathbb{E}(Y) = \frac{q}{q+1}$$

is the first moment of the Beta$(q, 1)$ distribution and

$$\mathbb{E}(X^{-1}) = \frac{1}{2}\sqrt{\frac{\pi}{\theta}}$$

is the first inverse moment of the IR(θ) distribution given in (1.6). □

Regular variation is a significant topic in extreme value theory (see Bingham [30]), and its formal definition is presented in what follows.

Definition 1. *A distribution function is called regularly varying at infinity with index $-\alpha$ if*

$$\lim_{x\to\infty} \frac{s(tx)}{s(x)} = t^{-\alpha}, \tag{2.8}$$

where the parameter $\alpha \geq 0$ is called the tail index.

We now show that the survival function of the SIR distribution is regularly varying, as stated in the following result.

Proposition 8. *If $Z \sim$ SIR(θ, q), then its survival function has regularly varying tails.*

Proof. From the previous definition and L'Hôpital's rule, we get

$$\lim_{z\to\infty} \frac{s(tz)}{s(z)} = t^{-q} \lim_{z\to\infty} \frac{\int_{\frac{\theta}{t^2 z^2}}^{\infty} \exp(-t)\, t^{-q/2}\, dt}{\int_{\frac{\theta}{z^2}}^{\infty} \exp(-t)\, t^{-q/2}\, dt},$$

since

$$\lim_{z\to\infty} \frac{\theta}{t^2 z^2} = \lim_{z\to\infty} \frac{\theta}{z^2} = 0$$

the limit on the righthand side is then computed to complete the proof. □

As the SIR distribution is regularly varying, it has a heavy tail (see Feller [31]).

Propositions 1–8 provide the main structural properties of the SIR distribution. In particular, Propositions 1–3 characterize its density, mode, and distribution function, Proposition 4 provides a hierarchical representation that motivates the ECM estimation procedure developed in the next section, Proposition 5 establishes the connection with the classical inverse Rayleigh model, Propositions 6 and 7 provide moment expressions used for moment-based estimation and initialization of the iterative algorithm, and Proposition 8 establishes the heavy-tailed nature of the distribution through regular variation arguments.

3. Estimation

In this section, we discuss estimation methods based on the modified moment (MM) estimators and the ML estimators for the unknown model parameters based on a random sample $Z_1, \ldots, Z_n$ from $Z \sim$ SIR(θ, q).

3.1. Method of moments

We consider the MM estimation method. Next, we present the MM estimators for the parameters of θ and q, which are based on $\mathbb{E}(Z)$ and $\mathbb{E}(Z^{-1})$ given in (2.6) and (2.7), and their statistics

$$S = \frac{1}{n}\sum_{i=1}^{n} Z_i \quad \text{and} \quad R = \frac{1}{n}\sum_{i=1}^{n} Z_i^{-1}.$$

The MM estimators are found by solving the following equations: $S = \mathbb{E}(T)$ and $R = \mathbb{E}(T^{-1})$. From the first equation, the value of q is given by

$$q = \frac{S}{S - \sqrt{\pi\theta}}, \qquad \theta < \frac{S^2}{\pi}. \tag{3.1}$$

From the second equation, we obtain

$$R = \frac{1}{2}\left(\frac{\pi}{\theta}\right)^{1/2}\left(\frac{q}{q+1}\right). \tag{3.2}$$

Equation (3.1) expresses q as a function of θ. Substituting this expression into Eq (3.2) yields an equation depending only on θ. Solving this equation with respect to θ provides the estimator $\widehat{\theta_M}$,

$$\hat{\theta}_M = \left(\frac{2RS + \sqrt{2RS(2RS - \pi)}}{2\sqrt{\pi}R}\right)^2, \qquad RS > \frac{\pi}{2}. \tag{3.3}$$

The estimator $\widehat{q_M}$ is then obtained by substituting $\widehat{\theta_M}$ into Eq (3.1).

3.2. ML estimators

The log-likelihood function can be expressed as

$$\ell(\theta, q) = n\log(\theta) + n\log(q) - \log(\pi) - 3\log(z_i) + \sum_{i=1}^{n}\log\Big(E_{q/2}\Big(\frac{\theta}{z_i^2}\Big)\Big). \tag{3.4}$$

This expression is obtained directly by taking logarithms of the density function in Eq (2.2), assuming an independent random sample.

By setting the first derivatives with respect to each parameter equal to zero, we obtain

$$\sum_{i=1}^{n}\frac{E_{q/2-1}\left(\frac{\theta}{z_i^2}\right)}{z_i^2\, E_{q/2}\left(\frac{\theta}{z_i^2}\right)} = \frac{n}{\theta}, \tag{3.5}$$

$$\sum_{i=1}^{n}\frac{E_{q/2+1}\left(\frac{\theta}{z_i^2}\right)}{E_{q/2}\left(\frac{\theta}{z_i^2}\right)} = \frac{2n}{q^2}.$$

The solution to this system of equations can be obtained using numerical methods such as the Newton-Raphson algorithm. Alternatively, these estimates can be found by directly maximizing the log-likelihood function, given in (3.4), using the optim subroutine of the R software (see R Core Team [32]).

As can be seen, the system of equations can be complex to solve. Therefore, we propose an alternative approach for finding the ML estimators. From now on, we will use the PDF of the SIR distribution in a reparameterized form. The following corollary shows the PDF of the SIR distribution reparameterized in terms of the mean.

Corollary 1. *Let $Z \sim \mathrm{SIR}(\mu, q)$. Then, the PDF of Z is given by*

$$f_Z(z;\mu,q) = \frac{\mu^2(q-1)^2}{\pi q z^3} E_{q/2}\left(\frac{1}{\pi}\left(\frac{\mu(q-1)}{qz}\right)^2\right), \quad z > 0, \tag{3.6}$$

where $\mu > 0$ and $q > 0$.

Proof. From (2.6), we have

$$\mu = \mathbb{E}(Z) = \frac{q\sqrt{\pi\theta}}{q-1},$$

then solving for θ we obtain

$$\theta = \frac{\left[\frac{\mu(q-1)}{q}\right]^2}{\pi}.$$

Substituting this value into (2.2) yields the result. □

3.3. An EM-type algorithm

In this section, we consider the ML estimation procedure based on an EM-type algorithm (see Dempster [33]).

For a sample $z_1, \ldots, z_n$ from the SIR model with associated covariates $\boldsymbol{x}_1, \ldots, \boldsymbol{x}_n$, respectively, the observed log-likelihood for $\boldsymbol{\psi} = (\boldsymbol{\beta}, q)$ can be written as

$$\ell(\boldsymbol{\psi}) = n\left(2\log(q-1) - \log(\pi) - \log(q)\right) + \sum_{i=1}^{n}\left\{\log(\mu_i) + \log\left[E_{q/2}\left(\frac{1}{\pi}\left(\frac{\mu_i(q-1)}{qz_i}\right)^2\right)\right]\right\}, \tag{3.7}$$

where $\mu_i = \exp(\mathbf{x}_i^\top\boldsymbol{\beta})$. Eq (3.3) is the log-likelihood of the reparameterized density given in Corollary 1, where the model is expressed in terms of its mean parameter. Direct maximization of (3.3) in

$$\mathbb{R}^p \times (1, +\infty)$$

with respect to $\boldsymbol{\psi}$ can be expensive in computational terms, considering that it depends on the integro-exponential function. For this reason, to facilitate the estimation process, we introduce latent variables $Y_1, \ldots, Y_n$ through the following hierarchical representation of the SIR model:

$$Z_i \mid Y_i = y_i;\ \mu_i, q \sim \mathrm{IR}\left(\frac{\mu_i^2(q-1)^2}{\pi y_i^2 q^2}\right) \quad \text{and} \quad Y_i \sim \mathrm{Beta}(q, 1).$$

Consequently, up to a constant, the complete log-likelihood function for $\boldsymbol{\psi} = (\boldsymbol{\beta}, q)$ is given by

$$\ell_c(\boldsymbol{\psi}) = 2\sum_{i=1}^{n}\boldsymbol{x}_i^\top\boldsymbol{\beta} + 2n\log(q-1) - n\log(q) + (q-3)\sum_{i=1}^{n}\log(Y_i) - \left(1 - \frac{1}{q}\right)^2\pi^{-1}\sum_{i=1}^{n}\exp\left(2\boldsymbol{x}_i^\top\boldsymbol{\beta}\right)Y_i^{-2}Z_i^{-2}.$$

Let $\widehat{v}_i = \mathbb{E}(Z_i^2 \mid Y_i = y_i;\ \mu_i, q)$, $\widehat{w}_i = \mathbb{E}(\log Z_i \mid Y_i = y_i;\ \mu_i, q)$ and $Q(\boldsymbol{\psi} \mid \widehat{\boldsymbol{\psi}}) = \mathbb{E}(\ell_c(\boldsymbol{\psi}) \mid \boldsymbol{\psi} = \widehat{\boldsymbol{\psi}})$. With those definitions, we have that

$$Q(\boldsymbol{\psi} \mid \widehat{\boldsymbol{\psi}}) = 2\sum_{i=1}^{n} \boldsymbol{x}_i^\top \boldsymbol{\beta} + 2n\log(q-1) - n\log(q) + (q-3)\sum_{i=1}^{n} \widehat{w}_i - \left(1 - \frac{1}{q}\right)^2 \pi^{-1} \sum_{i=1}^{n} \exp\left(2\boldsymbol{x}_i^\top \boldsymbol{\beta}\right) Z_i^{-2} \widehat{v}_i.$$

Note that

$$f(y_i \mid Z_i = z_i;\ \boldsymbol{\beta}, q) \propto y_i^{q-3} \exp\left(-\frac{\mu_i^2}{\pi z_i^2 y_i^2}\left(1 - \frac{1}{q}\right)^2\right) I_{(0,1)}(y_i).$$

This implies that

$$\widehat{v}_i = C_{10}(\boldsymbol{\psi};\ \boldsymbol{x}_i, z_i)/C_{00}(\boldsymbol{\psi};\ \boldsymbol{x}_i, z_i), \quad \widehat{w}_i = C_{01}(\boldsymbol{\psi};\ \boldsymbol{x}_i, z_i)/C_{00}(\boldsymbol{\psi};\ \boldsymbol{x}_i, z_i),$$

where

$$C_{rs}(\boldsymbol{\psi};\ \boldsymbol{x}_i, z_i) = \int_0^1 (\log u)^r\, u^{q+s-3}\, \exp\left(-\frac{\mu_i^2}{\pi\, z_i^2\, u^2}\left(1 - \frac{1}{q}\right)^2\right) du.$$

Since closed-form simultaneous updates for all parameters are not available, we adopt the ECM algorithm of Meng and Rubin [34]. The ECM procedure replaces the difficult joint maximization step of the EM algorithm with a sequence of simpler conditional maximization steps, yielding a computationally efficient estimation procedure while preserving the convergence properties of the EM framework. Therefore, the k-th iteration of the ECM algorithm is as follows:

- **E step**. For $i = 1, \ldots, n$, use $\widehat{\boldsymbol{\psi}}^{(k-1)}$, the estimate of $\boldsymbol{\psi}$ at the $(k-1)$-th iteration of the algorithm, to compute

$$\widehat{v}_i^{(k)} = C_{10}(\boldsymbol{\psi}^{(k-1)};\ \boldsymbol{x}_i, z_i)/C_{00}(\boldsymbol{\psi}^{(k-1)};\ \boldsymbol{x}_i, z_i), \quad \widehat{w}_i^{(k)} = C_{01}(\boldsymbol{\psi}^{(k-1)};\ \boldsymbol{x}_i, z_i)/C_{00}(\boldsymbol{\psi}^{(k-1)};\ \boldsymbol{x}_i, z_i).$$

- **CM step I**. Given $q^{(k-1)}$ and $\widehat{\mathbf{v}}^{(k)} = (\widehat{v}_1^{(k)}, \widehat{v}_2^{(k)}, \ldots, \widehat{v}_n^{(k)})$, maximize the expression

$$2\sum_{i=1}^{n} \boldsymbol{x}_i^\top \boldsymbol{\beta} - \left(1 - \frac{1}{q^{(k-1)}}\right)^2 \pi^{-1} \sum_{i=1}^{n} \exp\left(2\boldsymbol{x}_i^\top \boldsymbol{\beta}\right) Z_i^{-2} \widehat{v}_i^{(k)},$$

  with respect to $\boldsymbol{\beta}$ to update $\boldsymbol{\beta}^{(k)}$.
- **CM step II**. Given $\boldsymbol{\beta}^{(k)}$, $\widehat{\boldsymbol{v}}^{(k)}$, and $\widehat{\mathbf{w}}^{(k)} = (\widehat{w}_1^{(k)}, \widehat{w}_2^{(k)}, \ldots, \widehat{w}_n^{(k)})$, maximize the expression

$$2n\log(q-1) - n\log(q) + (q-3)\sum_{i=1}^{n} \widehat{w}_i^{(k)} - \left(1 - \frac{1}{q}\right)^2 \pi^{-1} \sum_{i=1}^{n} \exp\left(2\boldsymbol{x}_i^\top \boldsymbol{\beta}^{(k)}\right) Z_i^{-2} \widehat{v}_i^{(k)},$$

  with respect to q, subject to $q > 1$, to obtain $\widehat{q}^{(k)}$.

We repeat the E, CM-I, and CM-II steps until a given convergence condition is fulfilled. For instance, the difference between two consecutive iterations will be less than a pre-established value ($\epsilon = 10^{-4}$, for instance), i.e.,

$$\max\left\{|\beta_0^{(k)} - \beta_0^{(k-1)}|,\ |\beta_1^{(k)} - \beta_1^{(k-1)}|,\ \cdots,\ |\beta_p^{(k)} - \beta_p^{(k-1)}|,\ |q^{(k)} - q^{(k-1)}|\right\} < \epsilon.$$

Initial values for the ECM algorithm are taken as $\boldsymbol{\psi}^{(0)} = (\boldsymbol{\beta}^{(0)}, q^{(0)})$, where $\boldsymbol{\beta}^{(0)}$ denotes the maximum likelihood estimate under the IR regression model. Throughout this paper, we use $q^{(0)} = 2$. The proposed ECM algorithm is preferred over general-purpose optimization procedures because it exploits the hierarchical representation of the SIR distribution. While Newton-Raphson and related methods require evaluating gradients and Hessian matrices, the ECM algorithm avoids direct computation of second-order derivatives and guarantees that the likelihood increases across iterations. This property yields a stable and computationally attractive estimation procedure for the proposed model. Finally, the covariance matrix of $\widehat{\boldsymbol{\psi}}$ (the ML estimator of $\boldsymbol{\psi}$) can be estimated based on the Hessian matrix of the observed log-likelihood. The numDeriv package in R (see Gilber and Varadhan [35]) provides an accurate numerical approximation for such a matrix.

4. Simulation

In this section, we present a simulation study in order to assess the performance of the ML estimator obtained via the ECM algorithm described in Section 3.3. To drawn the data, we consider that each individual has a vector of available covariates, say $\boldsymbol{x}_i = (1, x_{1i}, x_{2i})$, where x_{1i} was drawn from the Bernoulli distribution with success probability of 0.5 and x_{2i} was drawn from the uniform model in the interval $(0, 10-5x_{1i})$ (in order to introduce a kind of correlation between x_{1i} and x_{2i}, more realistic). To choose the values of the vector of parameters $\boldsymbol{\beta} = (\beta_0, \beta_1, \beta_2)$, we consider that profiles $(1, 0, 0)$, $(1, 1, 0)$ and $(1, 1, 10)$ have associated means for the response variable m_0, m_1, and m_2. As $\mu_i = \exp\left(\mathbf{x}_i^\top \boldsymbol{\beta}\right)$, such conditions provide as solution

$$\beta_0 = \log(m_0), \qquad \beta_1 = \log(m_1) - \log(m_0), \qquad \beta_2 = \tfrac{1}{10}[\log(m_2) - \log(m_1)].$$

We consider four sample sizes: 20, 30, 50, and 100; three vectors for

$$(m_0, m_1, m_2)\colon \{(1,\ 0.75,\ 2),\ (0.5,\ 1.5,\ 1),\ (3,\ 2,\ 0.5)\},$$

and three values for the parameter q: 1.5, 2, and 3. For each of the 36 combinations of n, (m_0, m_1, m_2), and q, we have drawn 1,000 samples of size n considering $y_i \sim \mathrm{SIR}(\mu_i, q)$, $i = 1, \ldots, n$. Then, the parameters were estimated through the ECM algorithm. We report the estimated bias (Bias), the mean of the standard errors (SE) obtained from the Hessian matrix, and the RMSE. Note that the bias of all parameters decreases, and the SE and RMSE terms are closer as n increases, suggesting that the estimators are consistent.

Overall, the simulation results in Table 1 indicate that the ECM algorithm yields stable ML estimates across all scenarios considered. As the sample size increases, the bias, standard errors, and RMSE values decrease, supporting the consistency of the estimation procedure and illustrating its satisfactory finite-sample performance. Although the shape parameter q exhibits greater variability than the regression coefficients, particularly for smaller sample sizes, its estimation accuracy also improves as n increases. This behavior is expected, since q governs the distribution's tail behavior and is therefore more sensitive to sample fluctuations than the regression parameters. Moreover, the ECM algorithm converged successfully across all Monte Carlo replications, and no convergence failures or numerical instabilities were observed throughout the simulation study.

Table 1. Simulation study for the SIR regression model.

			$n = 20$			$n = 30$			$n = 50$			$n = 100$		
(m_0, m_1, m_2)	q	est.	Bias	SE	RMSE	Bias	SE	RMSE	Bias	SE	RMSE	Bias	SE	RMSE
$(1, 0.75, 2)$	1.5	q	0.351	1.994	1.488	0.305	1.296	1.230	0.242	0.900	0.848	0.164	0.467	0.446
		β_0	-0.143	0.753	0.678	-0.136	0.571	0.546	-0.133	0.469	0.446	-0.127	0.322	0.316
		β_1	-0.046	0.496	0.413	-0.038	0.378	0.324	-0.010	0.256	0.231	-0.006	0.167	0.160
		β_2	-0.001	0.095	0.084	0.000	0.067	0.062	0.000	0.051	0.047	0.001	0.035	0.032
	2	q	0.300	3.210	1.829	0.243	2.534	1.789	0.234	1.676	1.467	0.167	0.939	0.866
		β_0	-0.035	0.596	0.542	-0.029	0.429	0.409	-0.019	0.324	0.312	-0.013	0.238	0.235
		β_1	-0.024	0.442	0.375	-0.018	0.320	0.292	-0.011	0.232	0.213	-0.010	0.152	0.145
		β_2	-0.005	0.090	0.077	-0.001	0.061	0.057	0.000	0.046	0.043	-0.001	0.031	0.029
	3	q	0.385	4.778	2.184	0.315	4.240	2.084	0.279	3.582	1.969	0.153	2.384	1.808
		β_0	0.118	0.494	0.469	0.059	0.370	0.347	0.034	0.272	0.254	0.016	0.186	0.181
		β_1	-0.023	0.355	0.340	-0.012	0.268	0.257	-0.009	0.197	0.193	-0.003	0.141	0.138
		β_2	0.001	0.072	0.067	0.001	0.055	0.052	0.001	0.039	0.038	-0.002	0.027	0.027
$(0.5, 1.5, 1)$	1.5	q	0.328	1.770	1.416	0.316	1.328	1.296	0.223	0.893	0.880	0.157	0.490	0.484
		β_0	-0.152	0.792	0.702	-0.149	0.619	0.572	-0.148	0.446	0.426	-0.107	0.350	0.338
		β_1	-0.017	0.462	0.408	-0.007	0.357	0.321	-0.004	0.256	0.235	-0.003	0.165	0.164
		β_2	-0.002	0.094	0.085	0.000	0.068	0.062	0.002	0.047	0.045	0.001	0.033	0.032
	2	q	0.285	2.811	1.664	0.280	2.199	1.566	0.267	1.662	1.485	0.125	0.990	0.938
		β_0	-0.038	0.591	0.551	-0.031	0.427	0.418	-0.022	0.333	0.330	-0.021	0.229	0.228
		β_1	-0.024	0.452	0.387	-0.015	0.321	0.285	-0.014	0.245	0.222	-0.008	0.166	0.152
		β_2	0.003	0.092	0.074	0.000	0.074	0.060	-0.001	0.044	0.042	0.002	0.029	0.029
	3	q	0.384	4.970	2.032	0.272	4.380	2.018	0.186	3.362	1.891	0.165	2.471	1.806
		β_0	0.090	0.533	0.480	0.054	0.372	0.351	0.023	0.274	0.267	-0.008	0.180	0.176
		β_1	-0.018	0.374	0.348	-0.015	0.278	0.265	-0.001	0.197	0.194	-0.001	0.133	0.131
		β_2	0.003	0.078	0.071	0.000	0.055	0.051	0.001	0.041	0.039	-0.002	0.026	0.025
$(3, 2, 0.5)$	1.5	q	0.390	2.118	1.606	0.311	1.290	1.225	0.232	0.913	0.859	0.131	0.446	0.413
		β_0	-0.188	0.727	0.672	-0.155	0.591	0.575	-0.150	0.438	0.430	-0.083	0.327	0.320
		β_1	-0.025	0.469	0.405	-0.022	0.377	0.317	0.010	0.262	0.246	-0.002	0.171	0.165
		β_2	0.005	0.096	0.082	0.004	0.067	0.062	0.001	0.050	0.046	-0.001	0.034	0.032
	2	q	0.310	3.262	1.894	0.280	2.452	1.717	0.218	1.618	1.378	0.156	0.875	0.829
		β_0	-0.029	0.555	0.534	-0.017	0.437	0.417	-0.015	0.320	0.303	-0.008	0.232	0.227
		β_1	-0.025	0.373	0.357	-0.009	0.293	0.289	-0.008	0.214	0.213	-0.001	0.147	0.147
		β_2	0.000	0.090	0.077	-0.002	0.061	0.058	0.000	0.044	0.042	0.000	0.029	0.028
	3	q	0.328	4.817	2.038	0.243	4.042	1.999	0.178	3.374	1.904	0.150	2.265	1.689
		β_0	0.048	0.489	0.466	0.041	0.374	0.365	0.035	0.272	0.264	-0.002	0.182	0.179
		β_1	-0.022	0.367	0.337	-0.021	0.289	0.270	-0.010	0.209	0.203	0.007	0.139	0.137
		β_2	0.010	0.087	0.070	-0.001	0.062	0.052	0.000	0.045	0.039	-0.001	0.029	0.027

5. Application

The dataset analyzed in this study was obtained from the Department of Mines at the University of Atacama, Chile. It consists of measurements of the concentrations of neodymium (Nd), strontium (Sr), and zirconium (Zr) (in parts per million) for 86 mineral samples collected in Copiapó. This dataset has previously been analyzed in several methodological studies on flexible probability distributions and regression models (e.g., [9, 36–38]), making it an appropriate benchmark for evaluating new statistical methodologies. It was selected in the present study because the response variable is positive and exhibits pronounced right-skewness together with several relatively large observations, as well as characteristics frequently encountered in geochemical data and consistent with the heavy-tailed behavior that motivates the proposed SIR model. Furthermore, the dataset provides a realistic framework for assessing whether the additional flexibility introduced by the slash construction improves goodness of fit compared with existing inverse Rayleigh regression models.

The primary goal is to model the Nd concentration as a function of the Sr and Zr concentrations. Table 2 summarizes the descriptive statistics for Nd, whereas Figure 3 displays scatter plots of Nd against Sr and Zr. The descriptive statistics confirm the pronounced right-skewness of the response variable, while the scatter plots reveal a positive association between Nd and both covariates.

Table 2. Summary for neodymium dataset.

Mean	Median	Variance	cv	Skewness	Kurtosis
35.02	28.50	34.23	0.98	3.65	18.22

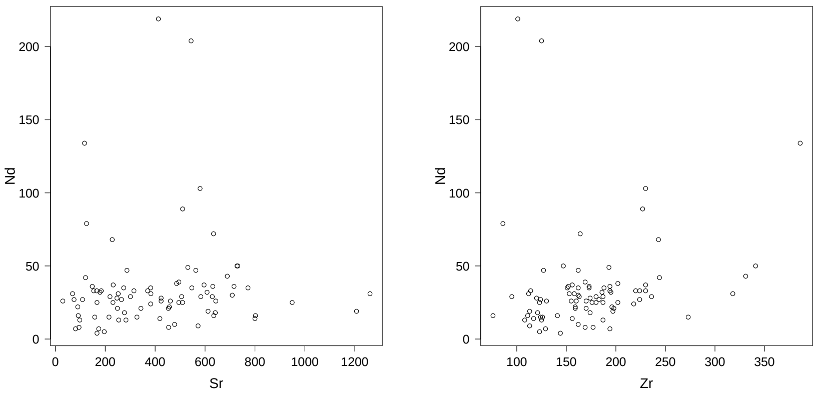

Figure 3. Plots for Nd versus Sr (left) and Nd versus Zr (right) for the mineral sample.

We compared the performance of the SIR regression model against several alternative specifications, namely, the reparameterized Gamma (RGA) model (see Nelder and Wedderburn [39]), the reparameterized Weibull (RWE) model, and the reparameterized Birnbaum-Saunders (RBS) model (Santos-Neto et al. [40]). We consider the relation

$$\log(\mu_i) = \beta_{\text{Intercept}} + \beta_{\text{Sr}}\, Sr_i + \beta_{\text{Zr}}\, Zr_i.$$

Model comparison was conducted using likelihood-based information criteria and randomized quantile residual diagnostics, since the main goal of this study is to evaluate the adequacy of competing distributional regression models rather than their predictive performance. Table 3 presents the estimated parameters, SE, AIC (Akaike information criterion; see Akaike [41]), and BIC (Bayesian information criterion; see Schwarz [42]) for the models under consideration. In general, the model that provides a better fit for the data is expected to yield smaller values of these criteria. Notably, all coefficients related to the distribution mean have lower standard errors in the SIR model than in the other competitors. Based on both AIC and BIC, the SIR regression model is the best-fitting for this dataset. We also computed 95% confidence intervals for the parameters $\beta_{\text{Intercept}}$, β_{Sr}, β_{Zn}, $\nu_{\text{Intercept}}$, and ν_{Zn}, which are (3.2624; 3.3405), (0.0005; 0.0011), (0.000289; 0.000290), (-8.6070;-5.7708), and (0.0224; 0.0244), respectively. Figure 4 displays the convergence behavior of the ECM algorithm for the mineral dataset. The observed-data log-likelihood increases monotonically and stabilizes rapidly, while the parameter estimates converge smoothly to their final values, providing empirical evidence of the stability and effectiveness of the proposed estimation procedure. To further assess the algorithm's sensitivity to the choice of initial values, Table 4 reports results obtained with several initial values for the shape parameter q. Although the number of iterations required for convergence varies across initializations, the algorithm consistently converges to the same maximum log-likelihood value and virtually identical parameter estimates. These results indicate that the proposed ECM algorithm is robust to the choice of the initial value of q in this application.

Table 3. Estimated parameters and SE for RGA, RBS, RWE, and SIR regression models in the mineral dataset.

Parameter	RGA		RBS		RWE		SIR	
	Estimate	SE	Estimate	SE	Estimate	SE	Estimate	SE
$\beta_{\text{Intercept}}$	3.1339	0.2459	3.2395	0.2645	2.8665	0.2509	2.4346	0.0018
β_{Sr}	0.0003	0.0003	0.0003	0.0003	0.0005	0.0003	0.0008	<0.0001
β_{Zr}	0.0016	0.0011	0.0011	0.0011	0.0027	0.0012	0.0052	<0.0001
σ	0.68779	0.0496	1.2929	0.0953	3.8262	0.5839	–	–
q	–	–	–	–	–	–	2.7162	0.0019
AIC	767.45		779.49		753.97		751.21	
BIC	777.27		789.31		763.78		761.02	

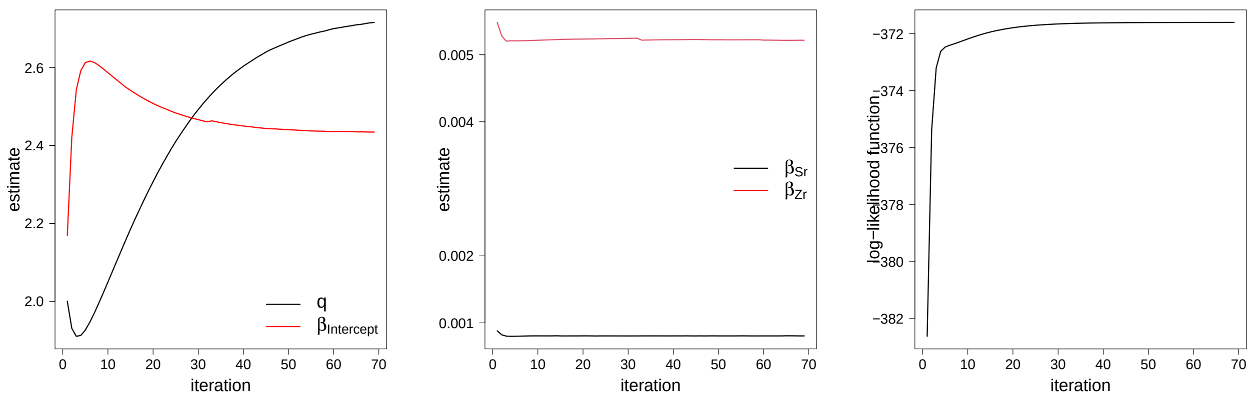

Figure 4. Convergence diagnostics for the ECM algorithm in the mineral data application. The figure displays the evolution of the parameter estimates and observed-data log-likelihood function throughout the iterative process.

Table 4. Sensitivity analysis of the ECM algorithm with respect to different initial values of the shape parameter q and the ML estimates for $\beta_{\text{Intercept}}$, β_{Sr}, and β_{Zr} taken as the ML estimates for the IR regression model.

$q^{(0)}$	iterations	log-likelihood	parameter estimates at convergence			
			q	$\beta_{\text{Intercept}}$	β_{Sr}	β_{Zr}
1.10	259	−371.6036	2.7163	2.4347	0.0008	0.0052
1.50	119	−371.6036	2.7162	2.4347	0.0008	0.0052
2.00	69	−371.6036	2.7162	2.4346	0.0008	0.0052
3.00	34	−371.6036	2.7162	2.4346	0.0008	0.0052
5.00	99	−371.6036	2.7163	2.4347	0.0008	0.0052

Figure 5 displays the estimated mean, its corresponding SE, and the estimated log-precision of Nd given Zn = (the median for Zn) and given Sr = (the median for Sr). In both cases, the estimated mean of Nd under the SIR model is lower than that obtained from the other competing models. We also note that the estimated standard errors are lower for the SIR regression model than for the others when $Zn = 68$ or $Sr = 382.5$ is fixed. On the other hand, the coefficients related to ϕ_i are not directly comparable across models, since in the RBS and RWE specifications the covariates enter through δ_i rather than ϕ_i. Nevertheless, we can compare the precision estimates obtained under the different models. It is worth noting that the estimated log-precisions for the RGA, RBS, and RWE models are similar to one another but differ considerably from those of the SIR model.

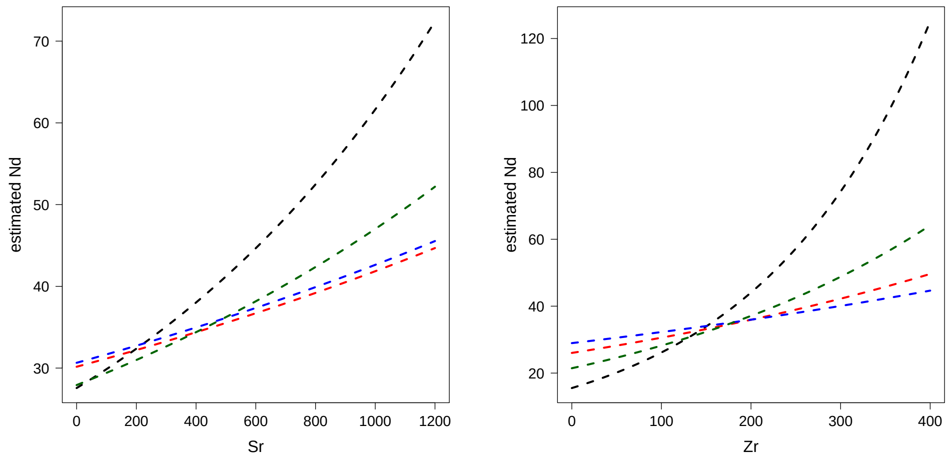

Figure 5. Estimated Nd, its standard error, and estimated log-precision for: i) Sr fixed at 382.5 ppm, and ii) Zn fixed at 68 ppm.

Figure 6 presents the randomized quantile residuals for the considered models. If a model is appropriate for the dataset, these residuals should behave as a random sample drawn from the standard normal distribution. Both the graphical diagnostics and the Kolmogorov-Smirnov (K-S) test indicate that the SIR model is the only one among the competing models that adequately describes the data. This finding provides empirical support for the suitability of the proposed SIR model for the analyzed dataset. Finally, the exponential of the parameters can be interpreted as shown in Table 5.

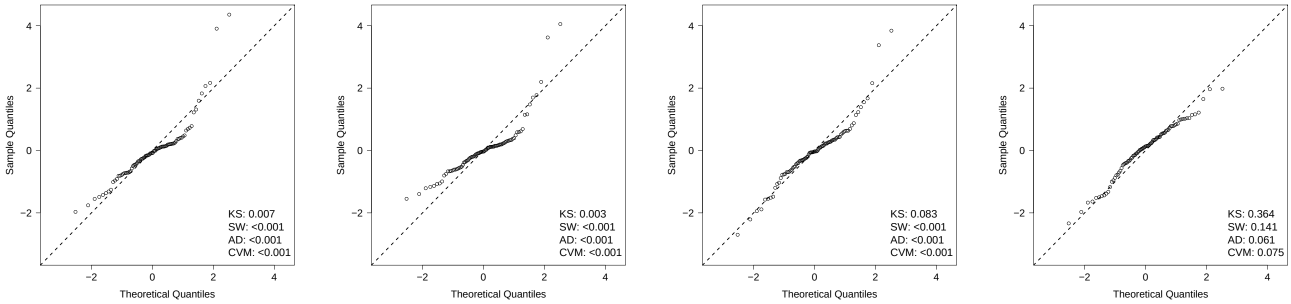

(a) (b) (c) (d)

Figure 6. Envelopes for the randomized quantile residuals from the RGA (a), RBS (b), RWE (c), and SIR (d) regression models for the mineral dataset. Also shown is the p-value from the K-S test assessing whether the residuals follow a standard normal distribution.

Table 5. Interpretations for the estimated parameters of the SIR regression model in the mineral dataset.

Quantity	Interpretation
$\exp(\widehat{\beta}_{\text{Intercept}}) \approx 27.15$	When both Sr and Zn are 0 ppm, the estimated quantity of Nd is 27.15 ppm.
$\exp(\widehat{\beta}_{Sr}) \approx 1.0008$	For a fixed level of Zn, a one-unit increase in Sr (in ppm) is associated with a 0.08% increase in the estimated quantity of Nd.
$\exp(\widehat{\beta}_{Zn}) \approx 1.0003$	For a fixed level of Sr, a one-unit increase in Zn (in ppm) is associated with a 0.03% increase in the estimated quantity of Nd.
$\exp(\widehat{\nu}_{\text{Intercept}}) \approx 0.0008$	When both Sr and Zn are 0 ppm, the estimated precision of Nd is 0.0008 ppm.
$\exp(\widehat{\beta}_{Zn}) \approx 1.0237$	For a fixed level of Sr, a one-unit increase in Zn (in ppm) is associated with a 2.37% increase in the estimated precision of Nd.

6. Conclusions

In this paper, we propose a novel extension of the inverse Rayleigh distribution, referred to as the SIR distribution. The proposed model is constructed using a stochastic representation based on the ratio of an inverse-Rayleigh random variable to an independent Beta random variable. This construction naturally extends the classical IR distribution by introducing an additional shape parameter, allowing greater flexibility in modeling data with heavy tails and varying degrees of skewness.

We derived the main distributional properties of the SIR model, including its PDF, CDF, survival function, and hazard rate. The hazard function can take a variety of shapes depending on the value of the shape parameter, making the model appealing for applications in reliability and survival analysis. Moreover, we establish a mixture representation and prove that the SIR distribution converges to the inverse Rayleigh model as the shape parameter tends to infinity.

From an inferential perspective, we developed an EM algorithm for ML estimation of the model parameters. The simulation study demonstrated that the proposed estimators perform well in terms of bias and mean squared error and exhibit the expected asymptotic behavior as the sample size increases.

The practical relevance of the proposed distribution is demonstrated using real mineral data, in which the model provided a better fit than competing models. This highlights its potential for modeling data characterized by high skewness and kurtosis, which are commonly encountered in applied fields.

Overall, the SIR distribution offers a flexible and analytically tractable alternative to the inverse Rayleigh model. Future research directions include Bayesian inference procedures for the model and further extensions incorporating additional shape parameters or covariate structures.

Author contributions

Héctor W. Gómez: Conceptualization of this study, methodology, writing—original draft preparation; Diego I. Gallardo: Conceptualization, investigation, software, writing—original draft preparation, writing—review and editing; Marcelo Bourguignon: Investigation, writing—original draft preparation; Osvaldo Venegas: Formal analysis, validation, writing—review and editing. All authors have read and approved the final version of the manuscript for publication.

Use of Generative-AI tools declaration

The authors declare they have not used Artificial Intelligence (AI) tools in the creation of this article.

Conflict of interest

All authors declare no conflicts of interest in this paper.

References

1. N. L. Johnson, S. Kotz, N. Balakrishnan, *Continuous univariate distributions*, New York: John Wiley & Sons, 1995.
2. W. H. Rogers, J. W. Tukey, Understanding some long-tailed symmetrical distributions, *Stat. Neerl.*, **26** (1972), 211–226. https://doi.org/10.1111/j.1467-9574.1972.tb00191.x
3. F. Mosteller, J. W. Tukey, *Data analysis and regression: a second course in statistics*, Reading, Mass.: Addison-Wesley Pub. Co., 1977.
4. K. Kafadar, A biweight approach to the one-sample problem, *J. Amer. Statist. Assoc.*, **77** (1982), 416–424. https://doi.org/10.1080/01621459.1982.10477827
5. J. Wang, M. G. Genton, The multivariate skew-slash distribution, *J. Stat. Plan. Inference*, **136** (2006), 209–220. https://doi.org/10.1016/j.jspi.2004.06.023
6. H. W. Gómez, F. A. Quintana, F. J. Torres, A new family of slash-distributions with elliptical contours, *Stat. Probab. Lett.*, **77** (2007), 717–725. https://doi.org/10.1016/j.spl.2006.11.006
7. H. W. Gómez, O. Venegas, Erratum to: "A new family of slash-distributions with elliptical contours" [Statist. Probab. Lett. 77 (2007) 717-725], *Stat. Probab. Lett.*, **78** (2008), 2273–2274. https://doi.org/10.1016/j.spl.2008.02.015
8. H. W. Gómez, J. F. Olivares-Pacheco, H. Bolfarine, An extension of the generalized Birnbaum-Saunders distribution, *Stat. Probab. Lett.*, **79** (2009), 331–338. https://doi.org/10.1016/j.spl.2008.08.014

9. N. M. Olmos, H. Varela, H. W. Gómez, H. Bolfarine, An extension of the half-normal distribution, *Stat. Pap.*, **53** (2012), 875–886. https://doi.org/10.1007/s00362-011-0391-4

10. N. M. Olmos, H. Varela, H. Bolfarine, H. W. Gómez, An extension of the generalized half-normal distribution, *Stat. Pap.*, **55** (2014), 967–981. https://doi.org/10.1007/s00362-013-0546-6

11. K. Cooray, M. M. A. Ananda, A generalization of the half-normal distribution with applications to lifetime data, *Commun. Stat. Theory Methods*, **37** (2008), 1323–1337. https://doi.org/10.1080/03610920701826088

12. J. M. Astorga, H. W. Gómez, H. Bolfarine, Slashed generalized exponential distribution, *Commun. Stat. Theory Methods*, **46** (2017), 2091–2102. https://doi.org/10.1080/03610926.2015.1032426

13. G. S. Mudholkar, D. K. Srivastava, M. Freimer, The exponentiated Weibull family: a reanalysis of the bus-motor-failure data, *Technometrics*, **37** (1995), 436–445. https://doi.org/10.1080/00401706.1995.10484376

14. R. D. Gupta, D. Kundu, Generalized exponential distributions, *Aust. N. Z. J. Stat.*, **41** (1999), 173–188. https://doi.org/10.1111/1467-842X.00072

15. Y. M. Gómez, H. Bolfarine, H. W. Gómez, Gumbel distribution with heavy tails and applications to environmental data, *Math. Comput. Simul.*, **157** (2019), 115–129. https://doi.org/10.1016/j.matcom.2018.10.003

16. V. N. Treyer, Inverse Rayleigh (IR) model, *Proc. USSR Acad. Sci.*, 1964.

17. V. G. Voda, On the inverse Rayleigh distributed random variable, *Rep. Stat. App. Res. JUSE*, **19** (1972), 13–21.

18. M. K. Gharraph, Comparison of estimators of location measures of an inverse Rayleigh distribution, *Egypt. Stat. J.*, **37** (1993), 295–309. https://doi.org/10.21608/esju.1993.426926

19. S. P. Mukherjee, S. S. Maiti, A percentile estimator of the inverse Rayleigh parameter, *IAPQR Trans.*, **21** (1996), 63–66.

20. H. A. Howlader, A. M. Hossain, O. Makhnin, Bayesian prediction bounds for Rayleigh and inverse Rayleigh lifetime models, *J. Appl. Stat. Sci.*, **17** (2009), 131–142.

21. A. Soliman, E. A. Amin, A. A. Abd-El Aziz, Estimation and prediction from inverse Rayleigh distribution based on lower record values, *Appl. Math. Sci.*, **4** (2010), 3057–3066.

22. A. M. Almarashi, M. M. Badr, M. Elgarhy, F. Jamal, C. Chesneau, Statistical inference of the half-logistic inverse Rayleigh distribution, *Entropy*, **22** (2020), 449. https://doi.org/10.3390/e22040449

23. E. Chiodo, M. Fantauzzi, G. Mazzanti, The compound inverse Rayleigh as an extreme wind speed distribution and its Bayes estimation, *Energies*, **15** (2022), 861. https://doi.org/10.3390/en15030861

24. R. A. Bakoban, A. M. Al-Shehri, A new generalization of the generalized inverse Rayleigh distribution with applications, *Symmetry*, **13** (2021), 711. https://doi.org/10.3390/sym13040711

25. C. Tanış, Transmuted lower record type inverse Rayleigh distribution: estimation, characterizations and applications, *Ric. Mat.*, **71** (2022), 777–802. https://doi.org/10.1007/s11587-022-00700-w

26. M. S. Khan, Modified inverse Rayleigh distribution, *Int. J. Comput. Appl.*, 87 (2014), 28–33.

27. M. Shala, F. Merovci, A new three-parameter inverse Rayleigh distribution: simulation and application to real data, *Symmetry*, **16** (2024), 634. https://doi.org/10.3390/sym16050634

28. E. Chiodo, L. P. Di Noia, Stochastic extreme wind speed modeling and Bayes estimation under the inverse Rayleigh distribution, *Appl. Sci.*, **10** (2020), 5643. https://doi.org/10.3390/app10165643

29. M. S. Milgram, The generalized integro-exponential function, *Math. Comput.*, **44** (1985), 443–458. https://doi.org/10.1090/S0025-5718-1985-0777276-4

30. N. H. Bingham, C. M. Goldie, J. L. Teugels, *Regular variation*, Cambridge: Cambridge University Press, 1987.

31. W. Feller, *An introduction to probability theory and its applications*, New York: John Wiley & Sons, Inc., 1971.

32. R Development Core Team, A language and environment for statistical computing, R version 4.1.0, 2021. Available from: `http://cran.csail.mit.edu/manuals.html`.

33. A. P. Dempster, N. M. Laird, D. B. Rubin, Maximum likelihood from incomplete data via the EM algorithm (with discussion), *J. R. Stat. Soc. Ser. B*, **39** (1977), 1–38. https://doi.org/10.1111/j.2517-6161.1977.tb01600.x

34. X. Meng, D. B. Rubin, Maximum likelihood estimation via the ECM algorithm: a general framework, *Biometrika*, **80** (1993), 267–278. https://doi.org/10.1093/biomet/80.2.267

35. P. Gilbert, R. Varadhan, *numDeriv: accurate numerical derivatives*, 2016.8-1, 2016. Available from: `https://cran.r-project.org/package=numDeriv`.

36. H. Bolfarine, H. W. Gómez, L. I. Rivas, The log-bimodal-skew-normal model: a geochemical application, *J. Chemom.*, **25** (2011), 329–332. https://doi.org/10.1002/cem.1378

37. B. C. Arnold, D. I. Gallardo, H. W. Gómez, A note on the Birnbaum-Saunders conditionals model, *Symmetry*, **13** (2021), 762. https://doi.org/10.3390/sym13050762

38. T. C. A. Leão, J. Leão, M. S. Lima, D. I. Gallardo, H. W. Gómez, Reparameterized slashed lognormal regression model: diagnostics and application to mineral data, *Chemom. Intell. Lab. Syst.*, **267** (2025), 105523. https://doi.org/10.1016/j.chemolab.2025.105523

39. J. A. Nelder, R. W. M. Wedderburn, Generalized linear models, *J. R. Stat. Soc. Ser. A*, **135** (1972), 370–384. https://doi.org/10.2307/2344614

40. M. Santos-Neto, F. J. A. Cysneiros, V. Leiva, M. Barros, A reparameterized Birnbaum-Saunders distribution and its moments, estimation and applications, *REVSTAT*, **12** (2014), 247–272. https://doi.org/10.57805/revstat.v12i3.153

41. H. Akaike, A new look at the statistical model identification, *IEEE Trans. Automat. Cont.*, **19** (1974), 716–723. https://doi.org/10.1109/TAC.1974.1100705

42. G. Schwarz, Estimating the dimension of a model, *Ann. Statist.*, **6** (1978), 461–464. https://doi.org/10.1214/aos/1176344136